Ready reckoners under vaccination based on POLYMOD contact surveys

Edwin van Leeuwen on behalf of the PHE modelling team

2021-04-22

Goal

Ready reckoners that highlight the impact of vaccination on the reproduction number, infection fatality ratio and total mortality of a potential wave after vaccination.

Overview

We estimate the reproduction number, infection fatality ratio (IFR) and total mortality for a number of scenarios and under different vaccination programmes. The different scenarios cover assumptions for school openings, number of contacts outside of the household and school, and effectiveness of the contact tracing programme. Contact rates were based on the POLYMOD contact survey. These results highlight that even at high coverage of 19 year and over there is still a significant probability that R is above 1 if schools are open and number of contacts were back to normal (Figure 1). The infection fatality ratio initially drops as more people are vaccinated (Figure 3). Similarly, if an outbreak occurs we would expect total mortality to be much reduced at high coverage (Figure 4).

Highlights

- Vaccination reduces the reproduction number, but is unlikely to reduce it to below 1 when contacts in school, work and leisure are back to normal levels (Figure 1).
- Vaccination reduces the infection fatality ratio up to a certain level, partly by protecting more at risk people from dying when infected and by reducing the relative number of infections in the older (more at risk) age groups. At high coverage in all age groups the mean age per infection will normalise again, resulting in a slight increase in the IFR (mortality **per** infection). This effect will be offset by the lower number of total infections in that case (Figure 4).
  - Similarly, opening schools would reduce the average age per infection and therefore the IFR. Again, this will be offset by the increase in the reproduction number and, therefore, total number of infections.

Caveats

- Existing natural immunity was kept constant going forward.
- For the total mortality estimate, behaviour and vaccine coverage were kept constant.
  - Vaccination was assumed to be leaky, i.e. it reduces the probability of infection per contact, but does not result in full protection.
- Number of contacts within the household were downscaled in order to match the full estimated reproduction number range over the course of this pandemic (0.6-3.5).
- Vaccine effectiveness assumptions were based on the SIREN study and assumed to be the same for all ages.

Table 1: Main assumptions used in the model.

Parameter	value	source
Susceptibility under 18	0.5 (0.35,0.75)	ONS; Munday et al. [2021]
VE dose 1	0.28 (0.14,0.42)	Hall et al. [2021]
VE dose 2	0.14 (0.03,0.24)	Hall et al. [2021]
VE vs mortality	0.49 (0.38,0.63)	Lopez Bernal et al. [2021]
Rel. trans. B.1.1.7	1.67 (1.43,1.9)	Davies et al. [2021]
Mortality by age		Levin et al. [2020]
Covid secure	0.25	
Doses per week	2062027	Median of last 5 weeks

- Mapping of POLYMOD contacts to current contact patterns involved many simplifying assumptions
  - Uncertainty in the contact matrices was carried over by bootstrapping the survey data.
- We did not take into account contact duration.
- Age distribution was strongly affected by estimates of susceptibility in the different age groups and the current attack rate in the different age groups.
- See table 1 for further assumptions around vaccine effectiveness, transmissibility etc.

Results

Figures 1 and 2 show that as work, leisure and other contacts increased, the effective reproduction number also increased, with the reproduction number still possibly being above 1 even at high vaccine uptake. As expected, keeping schools open resulted in higher reproduction numbers than having schools closed, but there was significant uncertainty in the level of impact of schools closing/opening. Contact tracing further reduced transmission.

Mortality per 100,000 infections changed depending on the vaccine coverage (Figure 3). Initially, the IFR dropped due to (1) reduction in mortality in the vaccinated at risk age groups and (2) having relatively more cases in the less at risk age groups. As vaccination in those (the less at risk) age groups increased the second cause became less important and mortality per infection rose again. Of course, the simultaneuous reduction in total incidence would still result in lower overall mortality (Figure 4).

Figure 4 shows the predicted mortality in England if a wave occurs after completion of different vaccination programmes. Total mortality dropped as vaccination increased, but sharply increased as work and leisure contacts increased. Even after full vaccination there was still a significant probability of an outbreak occurring, resulting in mortality, but it was much reduced compared to lower vaccination levels.

Currently a significant part of the adult population has been vaccinated, but achieving the necessary coverage in the rest of the population still poses a significant challenge. To get an indication on the timing of the different vaccination scenarios we calculated the rate of uptake under a vaccination rate of 2 million per week (Figure S2). Under such a vaccination rate we would expect all adults to be vaccinated with 1 dose by the end of July/beginning of August, with the second dose roll-out finishing 3 months later.

Methods

Mortality estimates by age group were based on previous IFR estimates [Levin et al., 2020]. Current natural immunity levels were taken from the PHE/Cambridge real time model [Birrell et al., 2020]. Vaccine efficacy against infection (susceptibility) was based on the SIREN analysis [Hall et al., 2021]. Vaccination uptake data was from 2021-04-01. Susceptibility for children was based on the ONS estimates (ONS 0.5 [0.35-0.75]; [Munday et al., 2021]). The age distribution of infections was then based on the (normalised) dominant eigenvector of the next generation matrix. For the main assumptions see Table 1.

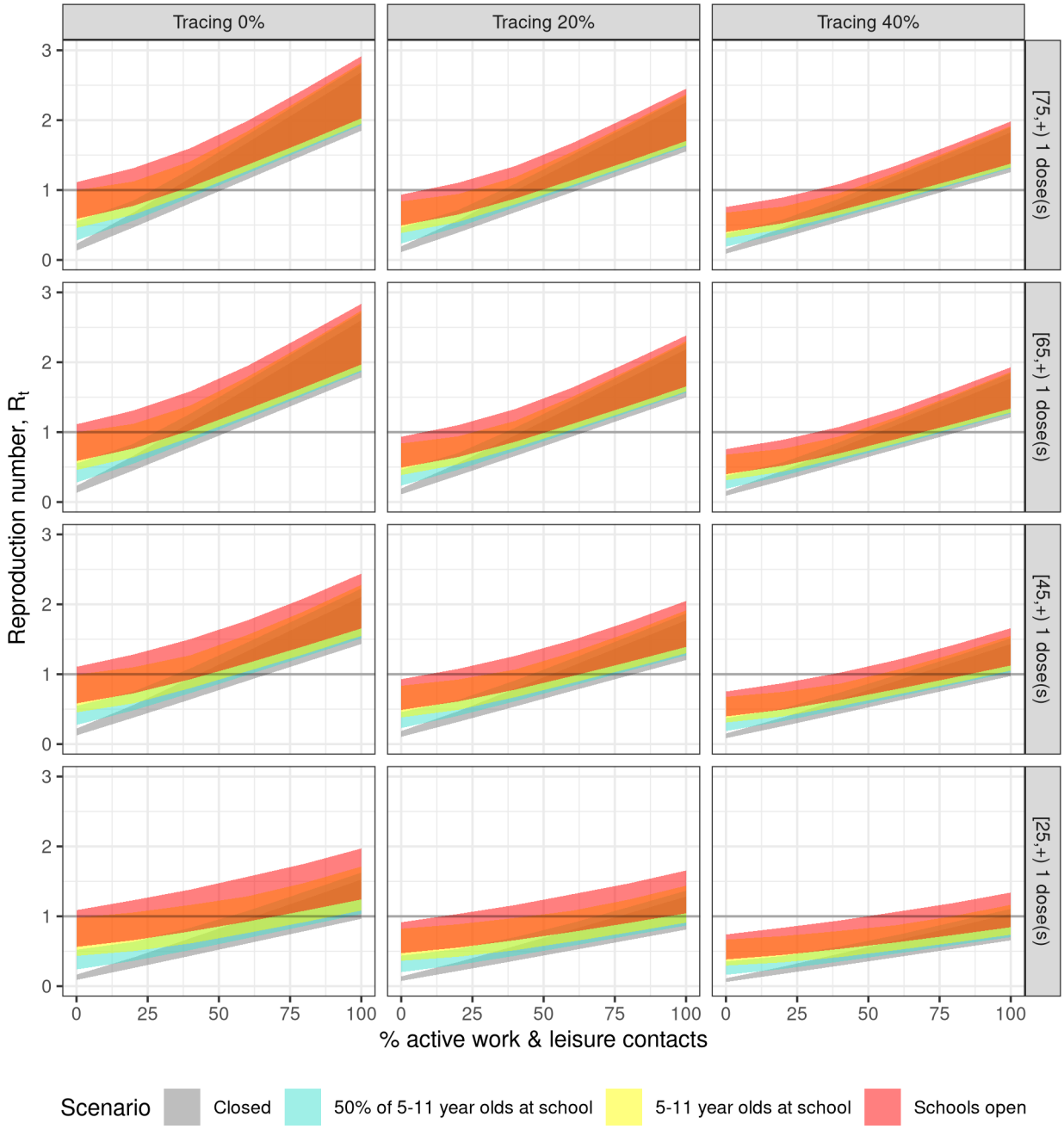

Figure 1: Ready reckoners for different vaccination coverage levels (rows). As work, leisure and other contacts increased (x-axis), the effective reproduction number also increased, with the reproduction number still possibly being above 1 even at higher vaccine uptake. As expected, having the schools open resulted (red) in higher reproduction numbers than keeping schools closed (grey), but there was significant uncertainty in the level of impact of schools closing/opening. Contact tracing would further reduce transmission (columns).

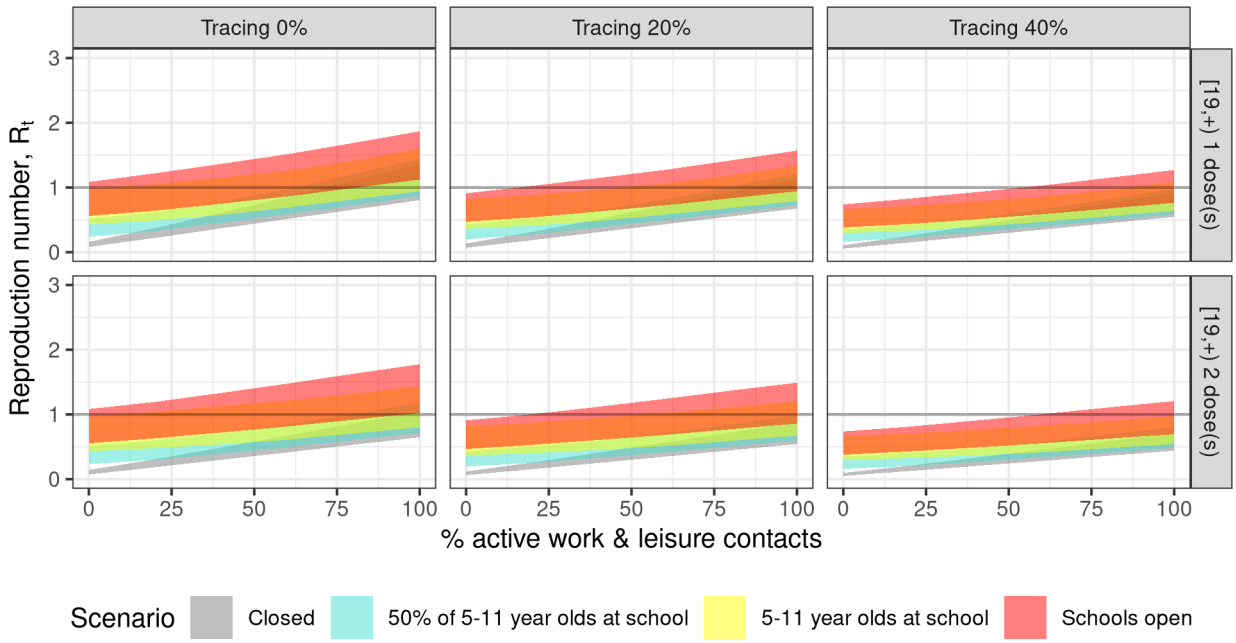

Figure 2: (Cont.) Ready reckoners for different vaccination coverage levels (rows). As work, leisure and other contacts increased (x-axis), the effective reproduction number also increased, with the reproduction number still possibly being above 1 even at higher vaccine uptake. As expected, having the schools open resulted (red) in higher reproduction numbers than keeping schools closed (grey), but there was significant uncertainty in the level of impact of schools closing/opening. Contact tracing would further reduce transmission (columns).

To capture the effect of NPIs on contact patterns we split contacts into unavoidable contacts (e.g. household contacts, some work contacts), avoidable (e.g. most leisure contacts) and school contacts. First, the POLYMOD contacts were split according to location (home, work, school, leisure, transport, otherplace; Mossong et al. [2008]). The home location was then further split into contacts with other household members and with visitors [van Leeuwen et al., 2020]. To create the contact matrix $C(\alpha, s)$ under a certain level of NPIs/adherence (α) and school attendance (s), we split the non-school contact matrices further into contacts that could be avoided/made safer (β_l) and unavoidable/constant contacts ($1-\beta_l$). The former were scaled by the α parameter, while the later were kept constant. This resulted in $c_{ij}(\alpha, s) = sc_{ij,\text{school}} + \sum_{l \neq \text{school}} (1-\alpha)\beta_l c_{ij,l} + (1-\beta_l)c_{ij,l}$. For this analysis we assumed that only contacts with household members were unavoidable.

Scaling contacts to the basic reproduction number

We assumed a basic reproduction number between $0.6 - 0.8$ when schools were closed and work and leisure contacts were reduced by 80, based on the first lockdown. The non-constant contacts (e.g. school, leisure, transport, otherplace and homevisit) were then scaled such that we had a basic reproduction number of $2.6 - 3.5$ when all contacts were as normal. For POLYMOD additional uncertainty was introduced by bootstrapping the raw data (using the socialmixr R package). We also assumed that effective contacts were reduced by 25 percent due to various covid security related measures (e.g. physical distancing, hand washing, PPE etc.). Finally, we assumed that transmission of the current dominant strain (B.1.1.7) is higher than the original strain [Davies et al., 2021].

Contact tracing (CT)

We used a simplified version of the method developped by Brooks-Pollock et al. [2020]. We assumed that 80% of index cases were symptomatic regardless of age [Buitrago-Garcia et al., 2020]. We then assumed that the specified percentage of contacts were traced before becoming infectious. For each interaction we assumed equal probability that either was the infector. This resulted in: $\hat{c}_{i,j} = (1 - 1/2(p_{si} + p_{sj})p_{ct})c_{i,j}$, where $c_{i,j}$

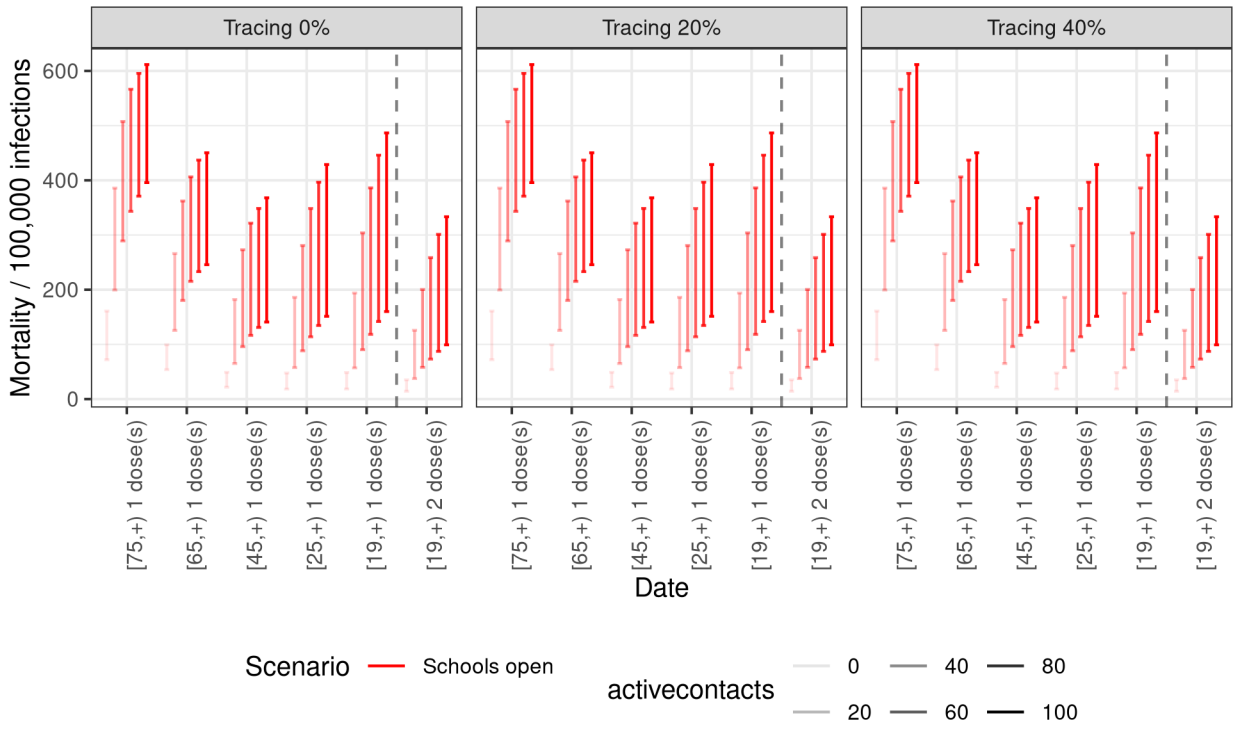

Figure 3: Mortality per 100,000 infections for different vaccination coverage scenarios. The results were grouped by vaccination programme (x-axis). The last group shows the results after completion of the vaccination programme (vaccinating everyone over 18 year old with two doses). The offset lines represent different fractions of work and leisure contacts (0, 0.2, 0.4, 0.6, 0.8, 1). Initially the IFR dropped due to (1) reduction in mortality in the vaccinated at risk age groups and (2) having relatively more cases in the less at risk age groups. As vaccination in those (the less at risk) age groups increased this second cause became less important and mortality per infection rose again. Of course, the simultaneuous reduction in total incidence would still result in lower overall mortality (Figure 4).

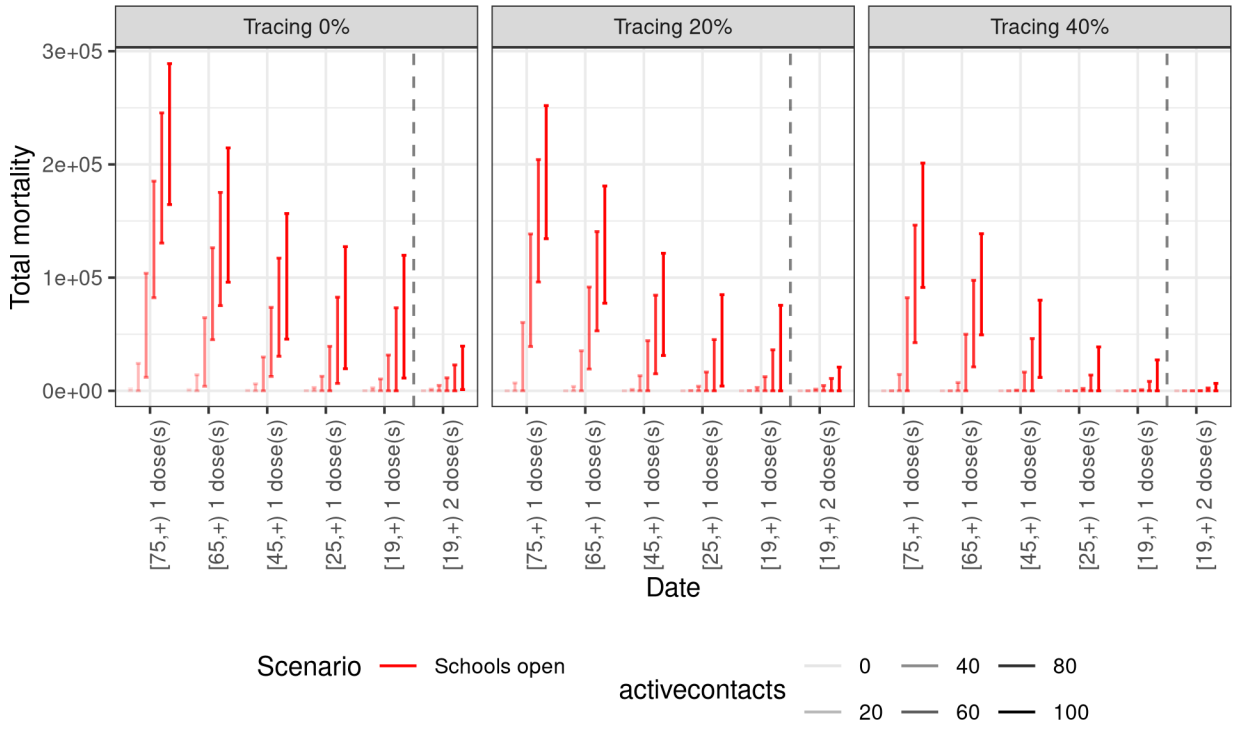

Figure 4: Predicted mortality in England if a wave occured after completion of different vaccination programmes. The results were grouped by vaccination programme (x-axis). The last group shows the results after completion of the vaccination programme (vaccinating everyone over 18 year old with two doses). The offset lines represent different fractions of work and leisure contacts (0, 0.2, 0.4, 0.6, 0.8, 1). Total mortality dropped as vaccination increased, but sharply increased as work and leisure contacts increased. Even after full vaccination there was still a significant probability of an outbreak occuring, resulting in mortality, but it was much reduced compared to lower vaccination levels.

was the number of contacts a person in age group i had with age group j, p_{ct} was the probability that the contact was traced before it could infect other people and p_{si} was the probability that an individual in age group i was symptomatic.

Final size

To get an indication of the total impact of different stages of the vaccination programme we estimated the size and mortality of a potential wave following vaccination. This assumed that behaviour stayed the same throughout the wave, and no further vaccination occurred during the outbreak. The final attack rate of the outbreak in a stratified population was calculated following Miller [2012]:

$$\pi(i) = 1 - \int_0^1 p_i(\sigma) e^{-\sum_j \sigma \Lambda_{ij} N_j \pi(j)} \mathrm{d}\sigma$$

with $\pi(i)$ the attack rate in group i, σ the susceptibility, $p_i(\sigma)$ the probability distribution for susceptibility within this group, $\Lambda_{ij} = \lambda \hat{c_{i,j}} / N_j$ the probability that an infected individual from group j infects an individual from group i, λ the infection probability per contact, and N_j the population size of group j. Vaccination resulted in changes to the susceptibility distribution in the age groups ($p_i(\sigma)$). In practice, we only considered four distinct values for susceptibility (fully susceptible, vaccinated with 1 dose, vaccinated with 2 doses and recovered), such that the integral simplified to the following sum: $\sum_k p_i(\sigma_k) e^{-\sum_j \sigma_k \Lambda_{ij} N_j \pi(j)}$.

Reproduction number

The reproduction number is the number of susceptibles infected by one typical infected [Diekmann et al., 1990, Miller, 2012]. In a stratified population the reproduction number is the dominant eigenvalue of the infection matrix ($A(\sigma)$), while the typical infected is the associated eigenvector ($x(\sigma)$) [Diekmann et al., 1990]. Here the matrix represents the rate with which an infected from group j infects someone in group i and can be defined as follows:

$$a_{ij} = \int_0^1 \sigma p_i(\sigma) \Lambda_{ij} N_i \mathrm{d}\sigma = \langle \sigma_i \rangle \Lambda_{ij} N_i$$

with $\langle \sigma_i \rangle$ the expected susceptibiliy in group i.

Vaccination

We assumed vaccination was evenly split between previously infected and susceptibles. This will be skewed somewhat, because future infections are less likely in the vaccinated. With high uptake or low incidence during vaccination this effect should be negligible.

Table S1: Assumed maximum vaccine uptake by age group.

AgeGroup	value
$[0, 6)$	0.00
$[6, 12)$	0.00
$[12, 19)$	0.00
$[19, 25)$	0.80
$[25, 45)$	0.80
$[45, 65)$	0.90
$[65, 75)$	0.95
$[75, +)$	0.95

Appendix

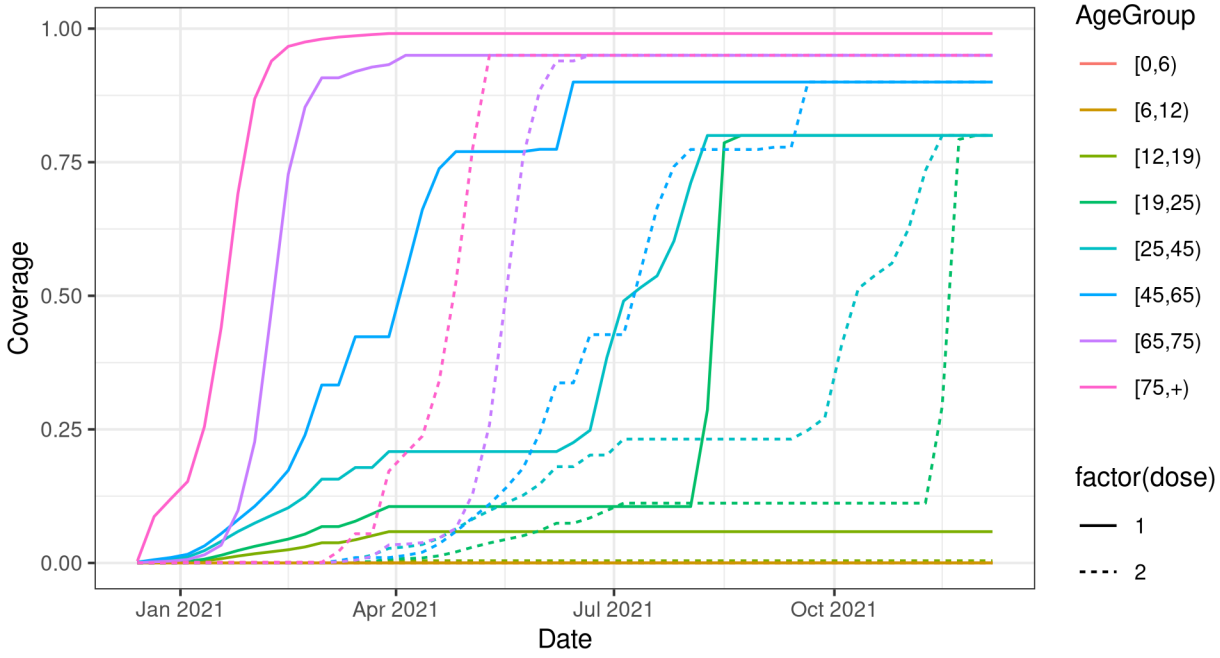

Figure S2: Vaccination coverage by age group and dose over time. The number of doses per week were based on the median uptake rate of the last 5 weeks ($\approx$ 2 million). Colours represent different age groups. Dotted lines represent the timing of a second dose assuming a 13 week delay between the 1st and 2nd dose. Note that administration of the 2nd dose could slow down administration of 1st doses in other age groups.

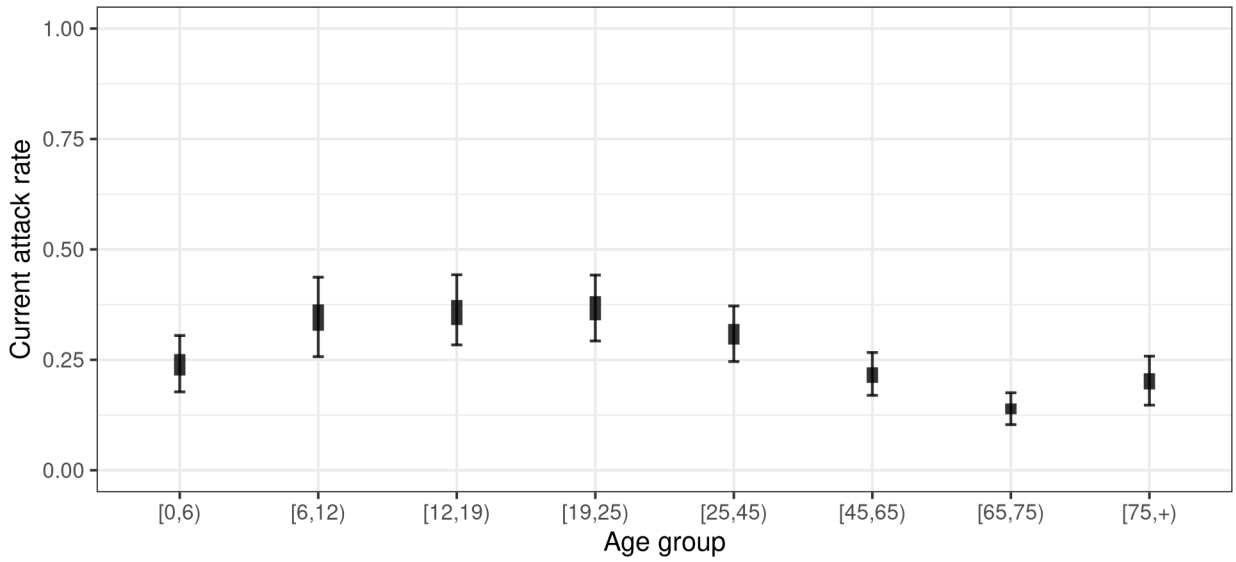

Figure S3: Current attack rate by age group. These rates were based on recent estimated attack rates in different age groups using the PHE/Cambridge model.

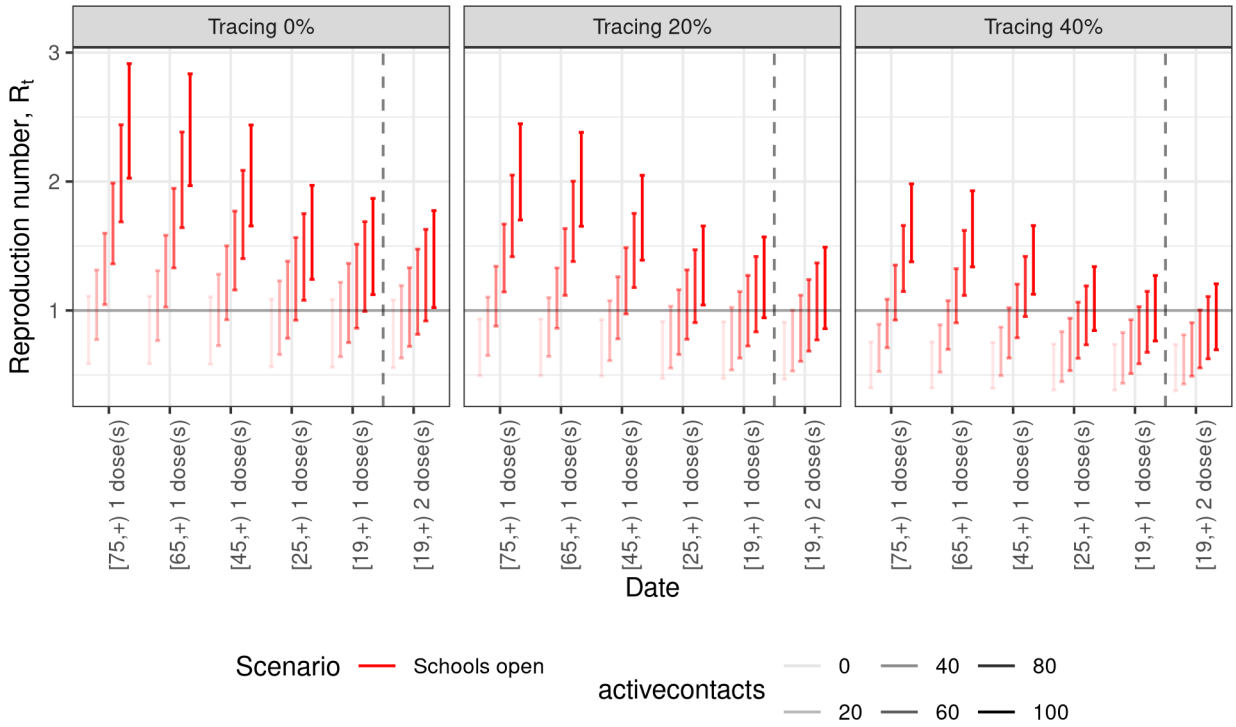

Figure S4: Reproduction number by vaccine uptake. The results here are the same as shown above (Figure 1), but summarised into one row. This made it easier to visually compare the differences in impact accross uptake levels, at the cost of some detail. The results were grouped by vaccination programme (x-axis). The last group shows the results after completion of the vaccination programme (vaccinating everyone over 18 year old with two doses). The offset lines represent different fractions of work and leisure contacts (0, 0.2, 0.4, 0.6, 0.8, 1). Reproduction number dropped as vaccination increased, but sharply increased as work and leisure contacts increased. Even after full vaccination there was still a significant probability of a reproduction number above 1, but it was much reduced compared to lower vaccination levels

References

Paul J. Birrell, Joshua Blake, Edwin van Leeuwen, Nick Gent, and Daniela De Angelis. Real-time Nowcasting and Forecasting of COVID-19 Dynamics in England: The first wave? *medRxiv*, page 2020.08.24.20180737, 2020. doi: 10/ghccp6.

Ellen Brooks-Pollock, Jonathan M. Read, Angela McLean, Matt J. Keeling, and Leon Danon. Using social contact data to predict and compare the impact of social distancing policies with implications for school re-opening. *medRxiv*, page 2020.07.25.20156471, July 2020. doi: 10/gjnkg8.

Diana Buitrago-Garcia, Dianne Egli-Gany, Michel J. Counotte, Stefanie Hossmann, Hira Imeri, Aziz Mert Ipekci, Georgia Salanti, and Nicola Low. Occurrence and transmission potential of asymptomatic and presymptomatic SARS-CoV-2 infections: A living systematic review and meta-analysis. *PLoS Med*, 17(9): e1003346, September 2020. ISSN 1549-1676. doi: 10/ghjkkt.

Nicholas G. Davies, Sam Abbott, Rosanna C. Barnard, Christopher I. Jarvis, Adam J. Kucharski, James D. Munday, Carl A. B. Pearson, Timothy W. Russell, Damien C. Tully, Alex D. Washburne, Tom Wenseleers, Amy Gimma, William Waites, Kerry L. M. Wong, Kevin van Zandvoort, Justin D. Silverman, CMMID COVID-19 Working Group1‡, COVID-19 Genomics UK (COG-UK) Consortium‡, Karla Diaz-Ordaz, Ruth Keogh, Rosalind M. Eggo, Sebastian Funk, Mark Jit, Katherine E. Atkins, and W. John Edmunds. Estimated transmissibility and impact of SARS-CoV-2 lineage B.1.1.7 in England. *Science*, March 2021. ISSN 0036-8075, 1095-9203. doi: 10/gh6x68.

O. Diekmann, J. A. P. Heesterbeek, and J. A. J. Metz. On the definition and the computation of the basic reproduction ratio R0 in models for infectious diseases in heterogeneous populations. *J. Math. Biol.*, 28(4): 365–382, June 1990. ISSN 1432-1416. doi: 10/btdjdj.

Victoria Jane Hall, Sarah Foulkes, Ayoub Saei, Nick Andrews, Blanche Oguti, Andre Charlett, Edgar Wellington, Julia Stowe, Natalie Gillson, Ana Atti, Jasmin Islam, Ioannis Karagiannis, Katie Munro, Jameel Khawam, The SIREN Study Group, Meera A. Chand, Colin Brown, Mary E. Ramsay, Jamie Lopez Bernal, and Susan Hopkins. Effectiveness of BNT162b2 mRNA Vaccine Against Infection and COVID-19 Vaccine Coverage in Healthcare Workers in England, Multicentre Prospective Cohort Study (the SIREN Study). SSRN Scholarly Paper ID 3790399, Social Science Research Network, Rochester, NY, February 2021.

Andrew T. Levin, William P. Hanage, Nana Owusu-Boaitey, Kensington B. Cochran, Seamus P. Walsh, and Gideon Meyerowitz-Katz. Assessing the age specificity of infection fatality rates for COVID-19: Systematic review, meta-analysis, and public policy implications. *Eur J Epidemiol*, 35(12):1123–1138, December 2020. ISSN 1573-7284. doi: 10/gh7jkf.

Jamie Lopez Bernal, Nick Andrews, Charlotte Gower, Julia Stowe, Chris Robertson, Elise Tessier, Ruth Simmons, Simon Cottrell, Richard Robertson, Mark O'Doherty, Kevin Brown, Claire Cameron, Diane Stockton, Jim McMenamin, and Mary Ramsay. Early effectiveness of COVID-19 vaccination with BNT162b2 mRNA vaccine and ChAdOx1 adenovirus vector vaccine on symptomatic disease, hospitalisations and mortality in older adults in England. Preprint, Infectious Diseases (except HIV/AIDS), March 2021.

Joel C. Miller. A note on the derivation of epidemic final sizes. *Bull Math Biol*, 74(9):2125–2141, September 2012. ISSN 0092-8240. doi: 10/f38ds4.

J. Mossong, N. Hens, M. Jit, P. Beutels, K. Auranen, R. Mikolajczyk, M. Massari, S. Salmaso, G. Tomba, J. Wallinga, J. Heijne, M. Sadkowska-Todys, M. Rosinska, and W. J. Edmunds. Social contacts and mixing patterns relevant to the spread of infectious diseases. *PLoS Med.*, 5(3):e74, 2008. ISSN 1549-1676. doi: 10/ch2stb.

James D. Munday, Christopher I. Jarvis, Amy Gimma, Kerry LM Wong, Kevin van Zandvoort, CMMID COVID-19 Working Group, Sebastian Funk, and W. John Edmunds. Estimating the impact of reopening schools on the reproduction number of SARS-CoV-2 in England, using weekly contact survey data. *medRxiv*, page 2021.03.06.21252964, March 2021. doi: 10/gh7xwn.

Edwin van Leeuwen, Frank G. Sandmann, Rosalind M. Eggo, PHE Joint modelling Group, and Peter J. White. Time use and social mixing during and around festive periods: Potential changes in the age distribution of COVID-19 cases from increased intergenerational interactions. *medRxiv*, page 2020.12.21.20248607, December 2020. doi: 10/ghqzpt.